# A One-Step Multi-Derivative Hybrid Block Method with Modified-Picard Iteration for the Solution of Second Order IVPs

Uthman O. Rufai, Precious Sibanda, and Sicelo P. Goqo

***Abstract*—This study presents a one-step multi-derivative hybrid block method (OSMDHBM) of order ten, which incorporates third derivatives for the solution of linear and nonlinear second-order initial value problems (IVPs). The derivation incorporates a multi-step collocation and interpolation method, using an approximated power series as the basis function. The intra-step or off-step points are obtained from the derivative of a shifted Legendre polynomial (SLP) of degree four. The accuracy, consistency, and stability properties of the method are analyzed. The nonlinear IVPs are linearized using the modified Picard iteration method (MPIM). In order to demonstrate the superiority of the method, numerical experiments are presented. Comparisons are made between the numerical results obtained and results from other methods and similar schemes in the literature.**

***Index Terms*—Interpolation, Collocation, Hybrid block, Shifted Legendre polynomial, Modified Picard iteration.**

## I. Introduction

IN the last half-century, much attention has been focused on exploring and creating new techniques for numerically integrating IVPs related to second-order (2-order) differential equations (DEs) in the form:

$$y'' = f(x,\, y,\, y'), \qquad x \in [a,\, b], \tag{1}$$

subject to the initial conditions:

$$y(a) = y_n, \qquad y'(a) = \delta_n, \tag{2}$$

where $y_n$ and $\delta_n$ are known constants. Equation (1) is extensively used in various applied sciences, including orbital dynamics, circuit theory and chemical kinetics. Numerous strategies have been proposed for solving (1) directly, including linear multi-step methods to overcome the Dahlquist barrier by introducing intra-step points during formulation.

Linear multi-step methods have been extensively used to solve first-order (1-order) IVPs and are conventionally applied to solve higher-order (H-order) IVPs by initially converting the ODE into an equivalent 1-order system (see [1], [2]). In recent years, researchers have placed a significant emphasis on utilizing block hybrid methods (BHMs) to solve Equation (1) directly. Studies have shown that this direct approach is more effective than the method of converting H-order IVPs into a system of 1-order IVPs in terms of execution time, cost-effectiveness and accuracy (see, for instance [3]–[5]).

Seventh-order linear multi-step method was proposed in [6] and was implemented in either predictor-corrector or block mode, proving to be more efficient for solving (1). Orakwelu $et\ al.$ [7] presented an optimized two-step BHM with symmetric off-step points for the solution of (1). Hybrid Obrechkoff methods were developed to enhance the accuracy of approximation and have been demonstrated to achieve an order $k+2$ [8].

Enright [9] and Gupta [10] independently proposed a method called multi-derivative methods to solve H-order IVPs. Tumba $et\ al.$ [11] through a power series approach, developed a uniformly eight-order implicit second-derivative method combined with Taylor method for solving stiff ordinary differential equations of 2-order. Extensive research findings (see [12], [13]) indicate that multi-derivative methods not only achieve higher accuracy but also exhibit robust stability properties.

The aim of this study is to develop a OSMDHBM of order ten, which incorporates third-derivatives (3-Ds) to solve linear (L) and nonlinear (N) IVPs in the form (1). The N-IVPs are linearized using a MPIM. We examine the effectiveness and stability properties of the proposed OSMDHBM.

## II. Derivation of the OSMDHBM

A one-step 3-D method of the form:

$$y_{n+p_i} = y_n + h\chi_{i\,j}\delta_n + h^2\beta_{i\,j}f_n + h^2\left(\sum_{j=1}^{\Phi}\alpha_{i\,j}f_{n+p_j}\right) + h^3\tau_{i\,j}g_n + h^3\left(\sum_{j=1}^{\Phi}\gamma_{i\,j}g_{n+p_j}\right), \tag{3}$$

$$\delta_{n+p_i} = \delta_n + h\eta_{i\,j}f_n + h\left(\sum_{j=1}^{\Phi}\zeta_{i\,j}f_{n+p_j}\right) + h^2\omega_{i\,j}g_n + h^2\left(\sum_{j=1}^{\Phi}\xi_{i\,j}g_{n+p_j}\right), \qquad i = 2, 3, ...., \Phi, \tag{4}$$

is developed for solving (1) over an interval with $a \le x \le b$ which is partitioned as $a = x_0 < x_1 < x_2 < \cdots < x_{R-1} < x_R = b$. The step length is conventionally denoted as $h =$

Manuscript received February 2, 2023; revised August 21, 2023. This work was supported by University of Kwazulu-Natal, South Africa.

U. O. Rufai is a postgraduate student of School of Mathematics, Statistics and Computer Science, University of KwaZulu-Natal, Pietermaritzburg, South Africa. (email: rufaiuthman18@gmail.com)

P. Sibanda is a professor of School of Mathematics, Statistics and Computer Science, University of KwaZulu-Natal, Pietermaritzburg, South Africa. (email: SibandaP@ukzn.ac.za)

S. P. Goqo is an associate professor of School of Mathematics, Statistics and Computer Science, University of KwaZulu-Natal, Pietermaritzburg, South Africa. (email: goqos@ukzn.ac.za)

$x_{n+1}-x_n$ for $n = 1, 2, 3, \ldots, R-1$. The IVP (1) is solved within the intervals $[x_n, x_{n+1}]$, using the initial values $y(x_n)$ and $y'(x_n)$ for $n = 0, 1, \ldots, R-1$. To improve the method's accuracy, $\Phi - 1$ off-step points are introduced. The set of points utilized in the solution process within each interval $[x_n, x_{n+1}]$ is given by

$$x_{n+p_0}, x_{n+p_1}, x_{n+p_2}, \ldots, x_{n+p_{M-1}}, x_{n+p_\Phi}, \tag{5}$$

where $x_{n+p_0} = x_n$ and $x_{n+p_\Phi} = x_{n+1}$. Set

$$y(x) \approx Y(x) = \sum_{\sigma=0}^{\Phi+\Psi} k_{n,\sigma}(x - x_n)^\sigma, \tag{6}$$

with the first, second and third derivatives given by

$$\delta(x) \approx Y'(x) = \sum_{\sigma=0}^{\Phi+\Psi} j\, k_{n,\sigma}(x - x_n)^{\sigma-1}, \tag{7}$$

$$\begin{aligned} Y''_{n+p_i} &= \sum_{\sigma=2}^{\Phi+\Psi} \sigma(\sigma-1)\, k_{n,\sigma}\,(x - x_n)^{\sigma-2} \\ &= f(x_{n+p_i}, y_{n+p_i}, \delta_{n+p_i}), \end{aligned} \tag{8}$$

$$\begin{aligned} Y'''_{n+p_i} &= \sum_{\sigma=2}^{\Phi+\Psi} \sigma(\sigma-1)(\sigma-2)\, k_{n,\sigma}\,(x - x_n)^{\sigma-3} \\ &= g(x_{n+p_i}, y_{n+p_i}, \delta_{n+p_i}, f_{n+p_i}), \\ & i = 2, 3, \ldots, \Phi, \end{aligned} \tag{9}$$

where $k_{n,\sigma}$ are unknown coefficients in the interval $[x_n, x_{n+1}]$ to be determined from a system of $\Phi + \Psi$ equations with unknowns generated from (8) and (9), and $\Psi = \Phi + 1$.

Apply the initial conditions:

$$\begin{aligned} Y(x_n) &= k_{n,0} = y_n, \\ Y'(x_n) &= k_{n,1} = \delta_n, \end{aligned} \tag{10}$$

and collocating at

$$x_{n+p_i} = x_n + hp_i, \qquad i = 2, 3, \ldots, \Phi.$$

When $\Phi = 5$, the points $p_i$ range from $p_1 = 0,\ p_2,\ p_3,\ p_4$, to $p_5 = 1$. The off-step points are $\phi = p_2,\ p_3$ and $p_4$. These off-step points are obtained from the derivative of a SLP of degree four, where

$$p_2 = \frac{1}{2} - \frac{\sqrt{21}}{14}, \qquad p_3 = \frac{1}{2}, \qquad p_4 = \frac{1}{2} + \frac{\sqrt{21}}{14}.$$

By solving equations (8) to (10) for all values of $M$. We obtain the unknown constants $k_{n,j}$. Substituting the coefficients $k_{n,j}$ into (6) and (7), we obtain a one-step 3-D method of the form (3) and (4). By evaluating (3) and (4) at $x_{n+p_i}$ for $i = 2, 3, \ldots, \Phi$, we obtain

$$\begin{aligned} \begin{bmatrix} y_{n+p_2} \\ y_{n+p_3} \\ \vdots \\ y_{n+p_\Phi} \end{bmatrix} &= y_n + h\delta_n \begin{bmatrix} \chi_{2,2} & \chi_{2,3} & \cdots & \chi_{2,\Phi} \\ \chi_{3,2} & \chi_{3,3} & \cdots & \chi_{3,\Phi} \\ \vdots & \vdots & \cdots & \vdots \\ \chi_{\Phi,2} & \chi_{\Phi,3} & \cdots & \chi_{\Phi,\Phi} \end{bmatrix} \\ &+ h^2 f_n \begin{bmatrix} \beta_{2,2} & \beta_{2,3} & \cdots & \beta_{2,\Phi} \\ \beta_{3,2} & \beta_{3,3} & \cdots & \beta_{3,\Phi} \\ \vdots & \vdots & \cdots & \vdots \\ \beta_{\Phi,2} & \beta_{\Phi,3} & \cdots & \beta_{\Phi,\Phi} \end{bmatrix} \\ &+ h^2 \begin{bmatrix} \alpha_{2,2} & \alpha_{2,3} & \cdots & \alpha_{2,\Phi} \\ \alpha_{3,2} & \alpha_{3,3} & \cdots & \alpha_{3,\Phi} \\ \vdots & \vdots & \cdots & \vdots \\ \alpha_{\Phi,2} & \alpha_{\Phi,3} & \cdots & \alpha_{\Phi,\Phi} \end{bmatrix} \begin{bmatrix} f_{n+p_2} \\ f_{n+p_3} \\ \vdots \\ f_{n+p_\Phi} \end{bmatrix} \\ &+ h^3 g_n \begin{bmatrix} \tau_{2,2} & \tau_{2,3} & \cdots & \tau_{2,\Phi} \\ \tau_{3,2} & \tau_{3,3} & \cdots & \tau_{3,\Phi} \\ \vdots & \vdots & \cdots & \vdots \\ \tau_{\Phi,2} & \tau_{\Phi,3} & \cdots & \tau_{\Phi,\Phi} \end{bmatrix} \\ &+ h^3 \begin{bmatrix} \gamma_{2,2} & \gamma_{2,3} & \cdots & \gamma_{2,\Phi} \\ \gamma_{3,2} & \gamma_{3,3} & \cdots & \gamma_{3,\Phi} \\ \vdots & \vdots & \cdots & \vdots \\ \gamma_{\Phi,2} & \gamma_{\Phi,3} & \cdots & \gamma_{\Phi,\Phi} \end{bmatrix} \begin{bmatrix} g_{n+p_2} \\ g_{n+p_3} \\ \vdots \\ g_{n+p_\Phi} \end{bmatrix}, \end{aligned} \tag{11}$$

and

$$\begin{aligned} \begin{bmatrix} \delta_{n+p_2} \\ \delta_{n+p_3} \\ \vdots \\ \delta_{n+p_\Phi} \end{bmatrix} &= \delta_n + hf_n \begin{bmatrix} \eta_{2,2} & \eta_{2,3} & \cdots & \eta_{2,\Phi} \\ \eta_{3,2} & \eta_{3,3} & \cdots & \eta_{3,\Phi} \\ \vdots & \vdots & \cdots & \vdots \\ \eta_{M,2} & \eta_{\Phi,3} & \cdots & \eta_{\Phi,\Phi} \end{bmatrix} \\ &+ h \begin{bmatrix} \zeta_{2,2} & \zeta_{2,3} & \cdots & \zeta_{2,\Phi} \\ \zeta_{3,2} & \zeta_{3,3} & \cdots & \zeta_{3,\Phi} \\ \vdots & \vdots & \cdots & \vdots \\ \zeta_{\Phi,2} & \zeta_{\Phi,3} & \cdots & \zeta_{\Phi,\Phi} \end{bmatrix} \begin{bmatrix} f_{n+p_2} \\ f_{n+p_3} \\ \vdots \\ f_{n+p_\Phi} \end{bmatrix} \\ &+ h^2 g_n \begin{bmatrix} \omega_{2,2} & \omega_{2,3} & \cdots & \omega_{2,\Phi} \\ \omega_{3,2} & \omega_{3,3} & \cdots & \omega_{3,\Phi} \\ \vdots & \vdots & \cdots & \vdots \\ \omega_{\Phi,2} & \omega_{\Phi,3} & \cdots & \omega_{\Phi,\Phi} \end{bmatrix} \\ &+ h^2 \begin{bmatrix} \xi_{2,2} & \xi_{2,3} & \cdots & \xi_{2,\Phi} \\ \xi_{3,2} & \xi_{3,3} & \cdots & \xi_{3,\Phi} \\ \vdots & \vdots & \cdots & \vdots \\ \xi_{\Phi,2} & \xi_{\Phi,3} & \cdots & \xi_{\Phi,\Phi} \end{bmatrix} \begin{bmatrix} g_{n+p_2} \\ g_{n+p_3} \\ \vdots \\ g_{n+p_\Phi} \end{bmatrix}. \end{aligned} \tag{12}$$

## III. Analysis of the Method

### A. Order of Accuracy

The local truncation error (LTE) associated with equation (3) can be defined in terms of a linear operator $\mathfrak{L}$ as

$$\begin{aligned} \mathfrak{L}[y(x_n);\, h] = \sum_{j=1}^{M} [&\alpha_{i\,j} y(x_n + p_j\, h) - h\beta_{i\,j} y'(x_n + p_j h) \\ &- h^2 \gamma_{i\,j} y''(x_n + p_j\, h) - h^3 \tau_{i\,j} y'''(x_n + p_j\, h)]. \end{aligned} \tag{13}$$

Assuming that $y(x_n)$ is sufficiently differentiable, the terms $y(x_n + p_j\, h),\ y'(x_n + p_j\, h),\ y''(x_n + p_j\, h)$ and

$y'''(x_n + p_j\, h)$ can be expanded using Taylor's series about $x_n$, yielding:

$$\begin{aligned}\mathfrak{L}[y(x_n);\, h] &= \hat{C}_0\, y(x_n) + \hat{C}_1 h\, y'(x_n) \\ &+ \hat{C}_2\, h^2\, y''(x_n) + \hat{C}_3\, h^3\, y'''(x_n) \\ &+ \ldots + \hat{C}_\mu\, h^\mu\, y^\mu(x_n) + \ldots,\end{aligned} \tag{14}$$

where the constant coefficients are $\hat{C}_\mu, \mu = 0,\, 1,\, 2,\, \ldots$. The method (3) has order $\mu$ if
$\mathfrak{L}[y(x);\, h] = O(h^{\mu+2})$, $\hat{C}_0 = \hat{C}_1 = \ldots = \hat{C}_\mu = \hat{C}_{\mu+1} = 0$ and $\hat{C}_{\mu+2} \neq 0$.

Therefore, $\hat{C}_\mu$ represents the order, $\hat{C}_{\mu+2}$ represents the error constant and $\hat{C}_{\mu+2}\, h^{\mu+2}\, y^{\mu+2}\,(x_n)$ represents the principal LTE at the point $x_n$. The LTE of the method are

$$\begin{aligned}\mathfrak{L}[y(x); h] = \Bigg\{ &\frac{1677 - 343\sqrt{21} y^{(12)}(x_n) h^{12}}{9467481952051200} + O(h^{13}), \\ &\frac{1677 + 343\sqrt{21} y^{(12)}(x_n) h^{12}}{9467481952051200} + O(h^{13}), \\ &\frac{y^{(12)}(x_n) h^{12}}{8739776102400} + O(h^{13}), \\ &\frac{y^{(12)}(x_n) h^{12}}{1971570585600} + O(h^{13}) \Bigg\}.\end{aligned}$$

We have

$$\hat{C}_0 = \hat{C}_1 = \ldots = \hat{C}_{10} = 0,$$

and the error constants are

$$\begin{aligned}\hat{C}_{12} = \Bigg( &\frac{1677 - 343\sqrt{21}}{9467481952051200}, \frac{1677 + 343\sqrt{21}}{9467481952051200}, \\ &\frac{1}{8739776102400}, \frac{1}{1971570585600} \Bigg)^T,\end{aligned}$$

indicating that the method has order $\mu = 10$.

### B. Stability Analysis

A matrix finite difference equation in block form can be used to express the OSMDHBM as

$$\begin{aligned}\tilde{A}_1 Y_{n+\Phi} = \tilde{A}_0 Y_n &+ h\, \tilde{\chi}_0\, \Delta_n + h^2\, \tilde{\alpha}_0\, F_{n+\Phi} \\ &+ h^2\, \tilde{\beta}_0\, F_n + h^3\, \tilde{\gamma}_0\, G_{n+\Phi} + h^3\, \tilde{\tau}_0\, G_n,\end{aligned} \tag{15}$$

$$\begin{aligned}\tilde{E}_1 \Delta_{n+\Phi} = \tilde{E}_0\, \Delta_n &+ h\, \tilde{\eta}_0\, F_n + h\, \tilde{\zeta}_1\, F_{n+\Phi} \\ &+ h^2\, \tilde{\omega}_0\, G_n + h^2\, \tilde{\xi}_1\, G_{n+\Phi},\end{aligned} \tag{16}$$

where

$$\begin{aligned}Y_{n+\Phi} &= (y_{n+p_2},\, y_{n+p_3},\, y_{n+p_4},\, y_{n+1})^T, \\ Y_n &= (y_{n-p_2},\, y_{n-p_3},\, y_{n-p_4},\, y_n)^T, \\ F_{n+\Phi} &= (f_{n+p_2},\, f_{n+p_3},\, f_{n+p_4},\, f_{n+1})^T, \\ F_n &= (f_{n-p_2},\, f_{n-p_3},\, f_{n-p_4},\, f_n)^T, \\ G_{n+\Phi} &= (g_{n+p_2},\, g_{n+p_3},\, g_{n+p_4},\, g_{n+1})^T, \\ G_n &= (g_{n-p_2},\, g_{n-p_3},\, g_{n-p_4},\, g_n)^T, \\ \Delta_{n+\Phi} &= (\delta_{n+p_2},\, \delta_{n+p_3},\, \delta_{n+p_4}\delta_{n+1})^T, \\ \Delta_n &= (\delta_{n-p_2},\, \delta_{n-p_3},\, \delta_{n-p_4},\, \delta_n)^T.\end{aligned} \tag{17}$$

The coefficients of the methods in (15) and (16) are provided as follows:

$$\tilde{A}_0 = \tilde{E}_0 = \begin{bmatrix}1 & 0 & 0 & 0\\ 1 & 0 & 0 & 0\\ 1 & 0 & 0 & 0\\ 1 & 0 & 0 & 0\end{bmatrix},\ \tilde{\beta}_0 = \begin{bmatrix}\beta_{2,2} & 0 & 0 & 0\\ \beta_{3,2} & 0 & 0 & 0\\ \beta_{4,2} & 0 & 0 & 0\\ \beta_{5,2} & 0 & 0 & 0\end{bmatrix},$$

$$\tilde{\chi}_0 = \begin{bmatrix}\chi_{2,2} & 0 & 0 & 0\\ \chi_{3,2} & 0 & 0 & 0\\ \chi_{4,2} & 0 & 0 & 0\\ \chi_{5,2} & 0 & 0 & 0\end{bmatrix},\ \tilde{A}_1 = \tilde{E}_1 = \begin{bmatrix}1 & 0 & 0 & 0\\ 0 & 1 & 0 & 0\\ 0 & 0 & 1 & 0\\ 0 & 0 & 0 & 1\end{bmatrix},$$

$$\tilde{\alpha}_1 = \begin{bmatrix}\alpha_{2,2} & \alpha_{2,3} & \alpha_{2,4} & \alpha_{2,5}\\ \alpha_{3,2} & \alpha_{3,3} & \alpha_{3,4} & \alpha_{3,5}\\ \alpha_{4,2} & \alpha_{4,3} & \alpha_{4,4} & \alpha_{4,5}\\ \alpha_{5,2} & \alpha_{5,3} & \alpha_{5,4} & \alpha_{5,5}\end{bmatrix},\ \tilde{\tau}_0 = \begin{bmatrix}\tau_{2,2} & 0 & 0 & 0\\ \tau_{3,2} & 0 & 0 & 0\\ \tau_{4,2} & 0 & 0 & 0\\ \tau_{5,2} & 0 & 0 & 0\end{bmatrix},$$

$$\tilde{\gamma}_1 = \begin{bmatrix}\gamma_{2,2} & \gamma_{2,3} & \gamma_{2,4} & \gamma_{2,5}\\ \gamma_{3,2} & \gamma_{3,3} & \gamma_{3,4} & \gamma_{3,5}\\ \gamma_{4,2} & \gamma_{4,3} & \gamma_{4,4} & \gamma_{4,5}\\ \gamma_{5,2} & \gamma_{5,3} & \gamma_{5,4} & \gamma_{5,5}\end{bmatrix},\ \tilde{\eta}_0 = \begin{bmatrix}\eta_{2,2} & 0 & 0 & 0\\ \eta_{3,2} & 0 & 0 & 0\\ \eta_{4,2} & 0 & 0 & 0\\ \eta_{5,2} & 0 & 0 & 0\end{bmatrix},$$

$$\tilde{\zeta}_1 = \begin{bmatrix}\zeta_{2,2} & \zeta_{2,3} & \zeta_{2,4} & \zeta_{2,5}\\ \zeta_{3,2} & \zeta_{3,3} & \zeta_{3,4} & \zeta_{3,5}\\ \zeta_{4,2} & \zeta_{4,3} & \zeta_{4,4} & \zeta_{4,5}\\ \zeta_{5,2} & \zeta_{5,3} & \zeta_{5,4} & \zeta_{5,5}\end{bmatrix},\ \tilde{\omega}_0 = \begin{bmatrix}\omega_{2,2} & 0 & 0 & 0\\ \omega_{3,2} & 0 & 0 & 0\\ \omega_{4,2} & 0 & 0 & 0\\ \omega_{5,2} & 0 & 0 & 0\end{bmatrix},$$

$$\tilde{\xi}_1 = \begin{bmatrix}\xi_{2,2} & \xi_{2,3} & \xi_{2,4} & \xi_{2,5}\\ \xi_{3,2} & \xi_{3,3} & \xi_{3,4} & \xi_{3,5}\\ \xi_{4,2} & \xi_{4,3} & \xi_{4,4} & \xi_{4,5}\\ \xi_{5,2} & \xi_{5,3} & \xi_{5,4} & \xi_{5,5}\end{bmatrix}.$$

The zero stability of the method concerns the stability of the difference system (15) as $h \to 0$. Thus, as (15) tends to

$$\tilde{A}_1 Y_{n+M} = \tilde{A}_0 Y_n.$$

The characteristics polynomial $\Omega(\psi)$ is given by

$$\Omega(\psi) = \det(\psi(\tilde{A}_1) - \tilde{A}_0) = \psi^3(\psi - 1),$$

and therefore, $\psi = 0$ and $\psi = 1$.

The OSMDHBM is zero stable for the roots $\Phi(\psi) = 0$ and satisfies $|\psi_j| \leq 1$. For the root with $|\psi_j| = 1$, it has a multiplicity of 1. Therefore, the OSMDHBM is zero stable, consistent with order $\mu > 1$ and also converges.

### C. Absolute Stability

The absolute stability region for the OSMDHBM can be defined as

$$\Re(z) = \{z \in \mathbb{C} : \mathcal{H}(z) < 1\}. \tag{18}$$

A region is said to have absolute stability (A-stable) if it contains the whole left half-plane.
Applying

$$y'' = \lambda^2 y, \qquad y''' = \lambda^3 y,$$

to the new method gives

$$Y_{n+M} = \mathcal{H}(z) Y_n, \qquad z = \lambda^2 h^2, \tag{19}$$

where the matrix $\mathcal{H}(z)$ is expressed as

$$\mathcal{H}(z) = \frac{\tilde{A}_0 + z\, \tilde{p}_0 + z^2\, \tilde{\beta}_0 + z^3\, \tilde{\tau}_0}{\tilde{A}_1 - z^2\, \tilde{\alpha}_1 - z^3\, \tilde{\gamma}_1}. \tag{20}$$

The stability function $\Re(z)$ can be determined by obtaining the dominant eigenvalues of the matrix $\mathcal{H}(z)$. The absolute stability region for this method is depicted in Figure 1.

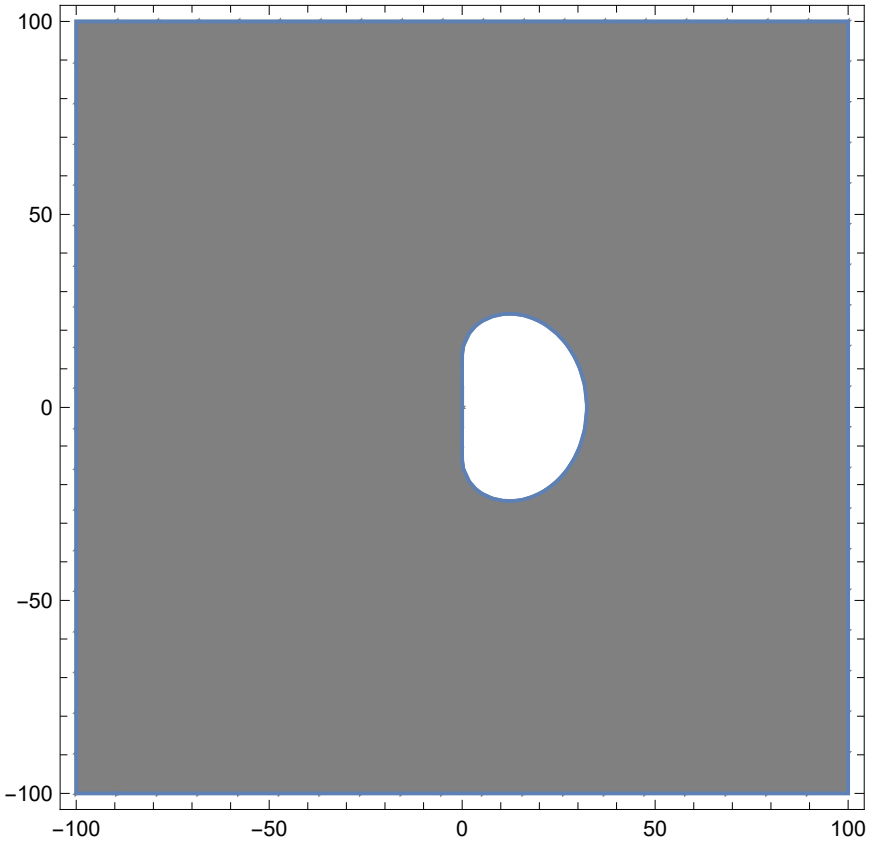


Fig. 1: Stability region

## IV. Implementation

### A. Linear Second-Order Differential Equations

Consider the general 2-order L-IVP of the form:

$$y'' = f(x,\, y,\, y') = \kappa(x) + \omega(x)y + \lambda(x)y'. \tag{21}$$

By differentiating (21), we obtain

$$y''' = g(t,\, y,\, y',\, y'') = \mathbf{l}(x) + \mathbf{q}(x)y + \mathbf{s}(x)y' + \mathbf{v}(x)y''. \tag{22}$$

Substituting (21) and (22) into (15) and (16) respectively, we obtain

$$\begin{bmatrix} \mathbf{A_{11}} & \mathbf{A_{12}} \\ \mathbf{A_{21}} & \mathbf{A_{11}} \end{bmatrix} \begin{bmatrix} Y_{n+\Phi} \\ \Delta_{n+\Phi} \end{bmatrix} = \begin{bmatrix} \mathbf{B_{1n}} \\ \mathbf{B_{2n}} \end{bmatrix}, \tag{23}$$

where

$$\begin{aligned}
\mathbf{A_{11}} &= \tilde{\mathrm{A}}_1 - h^2\,\tilde{\alpha}_1\,W_{n+\Phi} - h^2\,\tilde{\gamma}_1\,Q_{n+\Phi} \\
&\quad - h^3\,\tilde{\gamma}_1\,V_{n+\Phi}\,W_{n+\Phi}, \\
\mathbf{A_{12}} &= -h^2\,\tilde{\alpha}_1\,\Lambda_{n+\Phi} - h^3\,\tilde{\gamma}_1\,S_{n+\Phi} - h^3\,\tilde{\gamma}_1\,V_{n+\Phi}\Lambda_{n+\Phi}, \\
\mathbf{A_{21}} &= -h\,\tilde{\zeta}_1\,W_{n+\Phi} - h^2\,\tilde{\nu}_1\,Q_{n+\Phi} - h^2\,\tilde{\nu}_1\,v_{n+\Phi}\,W_{n+\Phi}, \\
\mathbf{A_{22}} &= \tilde{\mathrm{A}}_1 - h\,\tilde{\zeta}_1\,\Lambda_{n+\Phi} - h^2\,\tilde{\nu}_1\,S_{n+\Phi} \\
&\quad - h^2\,\tilde{\nu}_1\,V_{n+\Phi}\,\Lambda_{n+\Phi}, \\
\mathbf{B_{1n}} &= \tilde{\mathrm{A}}_0\,Y_n + h\,\tilde{\mathrm{p}}_0\,\Delta_n + h^2\,\tilde{\alpha}_1\,K_{n+\Phi} + h^2\,\tilde{\beta}_0\,F_n \\
&\quad + h^3\,\tilde{\tau}_0\,G_n + h^3\,\tilde{\gamma}_1\,L_{n+\Phi} + h^2\,\tilde{\gamma}_1\,V_{n+\Phi}\,K_{n+\Phi}, \\
\mathbf{B_{2n}} &= \tilde{\mathrm{E}}_0\,\Delta_n + h\,\tilde{\eta}_0\,F_n + h\,\tilde{\zeta}_1\,K_{n+\Phi} + h^2\,\tilde{\omega}_0\,G_n \\
&\quad + h^2\,\tilde{\nu}_1\,L_{n+\Phi} + h^2\,\tilde{\nu}_1\,V_{n+\Phi}\,K_{n+\Phi}.
\end{aligned}$$

We solve the L-system (23) to obtain the numerical solution (NS) for the L-IVPs.

### B. Nonlinear Second-Order Differential Equations

Consider a 2-order N-IVP of the form:

$$y'' = N(x,\, y,\, y') + L_1(x)y + L_2(x,\, y)y'. \tag{24}$$

We use a modified Picard-type iteration to solve (24). We evaluate all linear terms at the current iteration $(\iota + 1)$ and the nonlinear terms at the previous iteration $(\iota)$ to obtain

$$y'' = N(x,\, y_\iota,\, y'_\iota) + L_1(x)y_{\iota+1} + L_2(x,\, y_\iota)y'_{\iota+1}, \tag{25}$$

and

$$\begin{aligned}
y''' = {} & N(x, y_\iota,\, y'_\iota,\, y''_\iota) + L_1(x)y_{\iota+1} + L_2(x, y_\iota)y'_{\iota+1} \\
& + L_3(x, y_\iota,\, y'_\iota)y''_{\iota+1}.
\end{aligned} \tag{26}$$

This equation is in the linear form (21) and (22) with

$$\begin{aligned}
&\kappa(x) = N(x,\, y_\iota,\, y'_\iota), \quad \omega(x) = L_1(x), \\
&\lambda(x) = L_2(x,\, y_\iota),
\end{aligned}$$

and

$$\begin{aligned}
&\mathbf{q}(x) = L_1(x), \quad \mathbf{s}(x) = L_2(x,\, y_\iota), \\
&\mathbf{v}(x) = L_3(x, y_\iota,\, y'_\iota), \quad \mathbf{l}(x) = N(x,\, y_\iota,\, y'_\iota,\, y''_\iota).
\end{aligned}$$

We solve the L-system (23) to obtain the NS for the N-IVPs. In Section V, we demonstrate how this method can be applied to both 2-order L-IVPs and N-IVPs.

## V. Numerical Examples

In this section, numerical experiments are presented to demonstrate the application of the OSMDHBM and test its accuracy and effectiveness in solving these numerical examples.

*Example 1*

Consider the L-IVP:

$$y'' = 4y' - 8y + x^3, \quad y(0) = 2, \quad y'(0) = 4, \quad x \in [0, 1],$$

with exact solution:
$y(x) = e^{2x}(2\cos 2x - \frac{3}{64}\sin 2x) + \frac{3}{32}x + \frac{3}{16}x^2 + \frac{1}{8}x^3$.

In this example, the 3-D is given by

$$y''' = 4y'' - 8y' + 3x^2,$$

and the parameters are

$$\kappa(x, y, y') = x^3, \quad \omega(x) = -8, \quad \lambda(x) = 4,$$
$$l(x,\, y,\, y') = 3x^2, \quad q(x) = 0, \quad s(x) = -8, \quad v(x) = 4.$$

*Example 2*

A N-IVP given by

$$y'' = x(y')^2, \quad y(0) = 1, \quad y'(0) = \frac{1}{2},$$

with exact solution: $y(x) = 1 + \frac{1}{2} ln \left[\frac{2+x}{2-x}\right]$.

In this example, the 3-D is

$$y''' = (y')^2 + 2xy'y''.$$

The parameters are defined as follows:

$$\kappa(x,\, y_\iota,\, y'_\iota) = x(y'_\iota)^2, \quad \omega(x) = 0, \quad \lambda(x,\, y_\iota) = 0,$$
$$l(x,\, y_\iota,\, y'_\iota\, y''_\iota) = (y'_\iota)^2, \quad q(x) = 0, \quad s(x,\, y_\iota) = 0,$$
$$v(x,\, y_\iota,\, y'_\iota) = 2xy'_\iota.$$

*Example 3*

We consider a system of 2-order IVPs given by

$$y''_1 = y'_1, \qquad y_1(0) = 1, \qquad y'_1(0) = 1,$$
$$y''_2 = 2y'_1 + x\, y'_1, \qquad y_2(0) = 0, \qquad y'_2(0) = 1,$$

whose exact solutions are $y_1(x) = e^x$ and $y_2(x) = xe^x$.
In this example, the 3-Ds are

$$y'''_1 = y''_1 = y'_1$$
$$y'''_2 = (2 + x)y''_1 + y'_1 = (3 + x)y'_1.$$

The parameters are

$$\kappa_1(x,\, y_1,\, y_2,\, y'_1,\, y'_2) = 0, \quad \omega_1(x) = 0, \quad \lambda_1(x,\, y_1,\, y_2) = 1,$$
$$\kappa_2(x,\, y_1,\, y_2,\, y'_1,\, y'_2) = 2y'_1 + x\, y'_1, \quad \omega_2(x) = 0,$$
$$\lambda_2(x,\, y_1,\, y_2) = 0,$$
$$l_1(x,\, y_1,\, y_2,\, y'_1,\, y'_2,\, y''_1,\, y''_2) = 0, \quad q_1(x) = 0,$$
$$s_1(x,\, y_1,\, y_2) = 1, \quad v_1(x,\, y_1,\, y_2,\, y'_1,\, y'_2) = 0,$$
$$l_2(x,\, y_1,\, y_2,\, y'_1,\, y'_2,\, y''_1,\, y''_2) = (3 + x)y'_1,$$
$$q_2(x) = 0, \quad s_2(x,\, y_1,\, y_2) = 0, \quad v_2(x,\, y_1,\, y_2,\, y'_1,\, y'_2) = 0.$$

*Example 4*

We consider the following two body problem which was solved in [14] given by

$$y''_1 = \frac{-y_1}{\sqrt{y_1^2 + y_2^2}}, \qquad y_1(0) = 1, \qquad y'_1(0) = 0,$$
$$y''_2 = \frac{-y_2}{\sqrt{y_1^2 + y_2^2}}, \qquad y_2(0) = 0, \qquad y'_2(0) = 1,$$
$$x \in [0,\, 15\pi],$$

with exact solutions: $y_1(x) = \cos x$ and $y_2(x) = \sin x$.
In this example, the 3-Ds are

$$y'''_1 = \frac{-y'_1(y_2^2) + y_1 y_2 y'_2}{\left(\sqrt{y_1^2 + y_2^2}\right)^3}$$
$$y'''_2 = \frac{-y'_2(y_1^2) + y_1 y_2 y'_1}{\left(\sqrt{y_1^2 + y_2^2}\right)^3}.$$

The parameters are

$$\kappa_1(x,\, y_{1,\iota},\, y_{2,\iota},\, y'_{1,\iota},\, y'_{2,\iota}) = \frac{-y_{1,\iota}}{\sqrt{y_{1,\iota}^2 + y_{2,\iota}^2}}, \quad \omega_1(x) = 0,$$
$$\lambda_1(x,\, y_{1,\iota},\, y_{2,\iota}) = 0,$$
$$\kappa_2(x,\, y_{1,\iota},\, y_{2,\iota},\, y'_{1,\iota},\, y'_{2,\iota}) = \frac{-y_{2,\iota}}{\sqrt{y_{1,\iota}^2 + y_{2,\iota}^2}}, \quad \omega_2(x) = 0,$$
$$\lambda_2(x,\, y_{1,\iota},\, y_{2,\iota}) = 0,$$
$$l_1(x,\, y_{1,\iota},\, y_{2,\iota},\, y'_{1,\iota},\, y'_{2,\iota},\, y''_{1,\iota},\, y''_{2,\iota}) = \frac{-y'_{1,\iota}(y_{2,\iota}^2) + y_{1,\iota} y_{2,\iota} y'_{2,\iota}}{\left(\sqrt{y_{1,\iota}^2 + y_{2,\iota}^2}\right)^3},$$
$$q_1(x) = 0, \quad s_1(x,\, y_{1,\iota},\, y_{2,\iota}) = 0,$$
$$v_1(x,\, y_{1,\iota},\, y_{2,\iota},\, y'_{1,\iota},\, y'_{2,\iota}) = 0,$$
$$l_2(x,\, y_{1,\iota},\, y_{2,\iota},\, y'_{1,\iota},\, y'_{2,\iota},\, y''_{1,\iota},\, y''_{2,\iota}) = \frac{-y'_{2,\iota}(y_{1,\iota}^2) + y_{1,\iota} y_{2,\iota} y'_{1,\iota}}{\left(\sqrt{y_{1,\iota}^2 + y_{2,\iota}^2}\right)^3},$$
$$q_2(x) = 0, \quad s_2(x,\, y_{1,\iota},\, y_{2,\iota}) = 0,$$
$$v_2(x,\, y_{1,\iota},\, y_{2,\iota},\, y'_{1,\iota},\, y'_{2,\iota}) = 0.$$

## VI. Results and Discussion

In this section, we present the results obtained from implementing OSMDHBM with order ten and $\psi = 3$ for solving 2-order L-IVPs and N-IVPs. Table I–VII illustrate the computation time, absolute error, maximum error, maximum relative error, rate of convergence and number of function evaluations at selected points using the method. Figures 2–6 depict the absolute error and convergence error of the method. All the results were obtained using the number of partitions $R = \frac{b-a}{h}$, where $h$ represents the step size. The non-linear equations were solved using the MPIM. We compared our results with those obtained in ( [6], [14]–[17]).

The maximum relative error (MRE) and the rate of convergence (ROC) on the closed interval $[x_n, x_{n+1}]$ is defined as follows:

$$MRE = \max_{1 \le i \le \Phi} \frac{|y(x_{n+p_i}) - y_{n+p_i}|}{|y(x_{n+p_i})|},$$

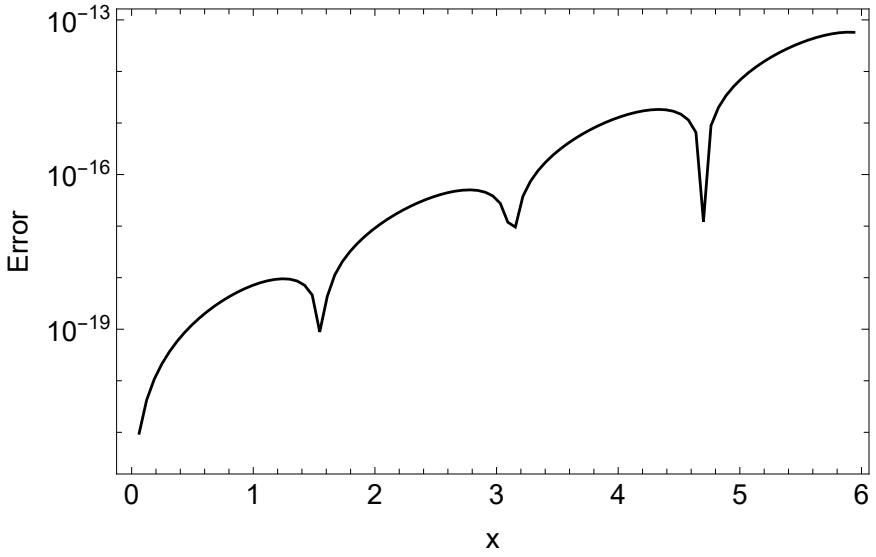


Fig. 2: Absolute error graph for $y$ when $\psi = 3$ at $R = 97$

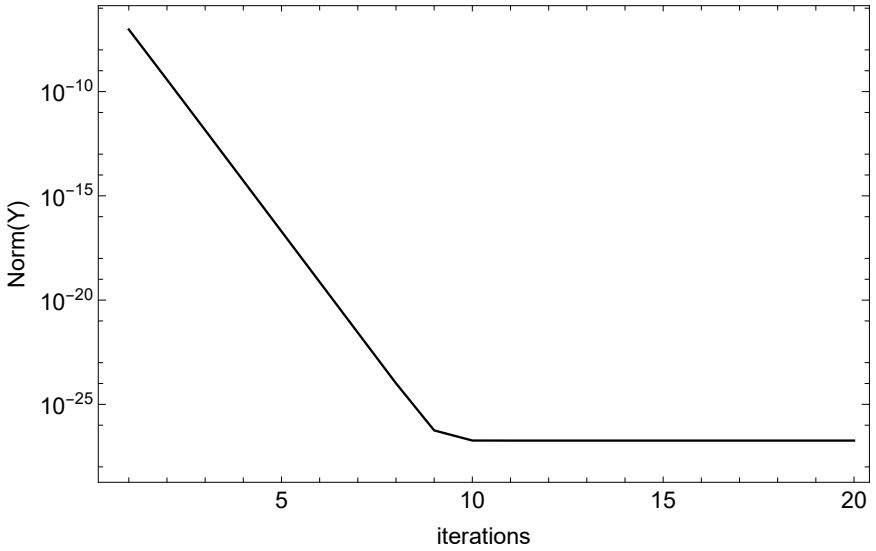


Fig. 3: Convergence graph for y when $\psi = 3$ at $h = \frac{1}{100}$

and

$$ROC = \log_2 \frac{MAE_{2h}}{MAE_h},$$

where $MAE$ is the maximum absolute error and $h$ is the step size.

TABLE I: MAXERR $(max_i|y(x_i) - y_i|)$ for Example 1

| $R$ | SOLMM [6] | BSSHA-BAP [16] $m = 5$ | OSMDHBM $\psi = 3$ | OSMDHBM CPU Time |
|---|---|---|---|---|
| 7 | 3.14 x $10^{-3}$ | 1.97 x $10^{-12}$ | 3.09 x $10^{-15}$ | 0.0011 |
| 13 | 1.40 x $10^{-5}$ | 1.36 x $10^{-14}$ | 6.34 x $10^{-18}$ | 0.002 |
| 25 | 5.07 x $10^{-8}$ | 7.25 x $10^{-17}$ | 9.16 x $10^{-21}$ | 0.0038 |
| 49 | 1.92 x $10^{-10}$ | 3.32 x $10^{-19}$ | 1.09 x $10^{-23}$ | 0.0077 |
| 97 | 5.31 x $10^{-12}$ | 1.41 x $10^{-21}$ | 1.18 x $10^{-26}$ | 0.0142 |

Table I displays the maximum error and computation time at different grid points ($R$) on the closed interval [0,1], obtained using the OSMDHBM and compared with the seventh-order linear multi-step method (SOLMM) [6] and the block single-step hybrid algorithms based on Bhaskara approximation points (BSSHA-BAP) [16] with five intra-step points. It observed that the OSMDHBM achieves superior convergence with a few intra-step points (three) used. However, as the number of partitions $R$ increases, the computation time for OSMDHBM convert to four decimal places also increases. In Table II, the maximum relative error, rate of convergence and number of function evaluations of the OSMDHBM are presented at different grid points ($R$) on the closed interval [0,1].

TABLE II: Maximum relative error, rate of convergence and number of function evaluations for OSMDHBM in Example 1

| $R$ | MRE | ROC | NF$_{eval}$ |
|---|---|---|---|
| 7 | 9.610 x $10^{-14}$ | 13.717 | 35 |
| 13 | 4.5034 x $10^{-17}$ | 13.687 | 65 |
| 25 | 4.2680 x $10^{-20}$ | 13.677 | 125 |
| 49 | 3.3881 x $10^{-22}$ | 13.675 | 245 |
| 97 | 2.5304 x $10^{-25}$ | 13.674 | 485 |

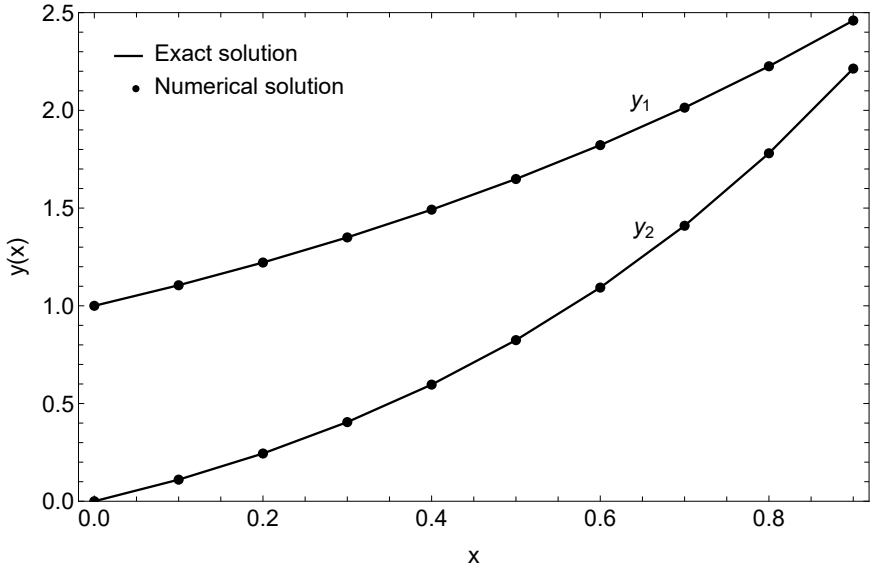


Fig. 4: Numerical vs Exact solution for $y_1$ and $y_2$ when $\psi = 3$ at $h = \frac{1}{10}$

TABLE III: Absolute error for Example 2 when $\psi = 3$ at $h = \frac{1}{100}$

| | BTSHM-BP [7] | OTSBHM [7] | OSMDHBM |
|---|---|---|---|
| $x$ | $m = 5$ | $m = 5$ | $\psi = 3$ |
| 0.1 | 2.22 x $10^{-16}$ | 2.22 x $10^{-16}$ | 1.02 x $10^{-31}$ |
| 0.2 | 0 | 0 | 8.73 x $10^{-31}$ |
| 0.3 | 2.22 x $10^{-16}$ | 0 | 3.34 x $10^{-30}$ |
| 0.4 | 0 | 0 | 9.48 x $10^{-30}$ |
| 0.5 | 4.44 x $10^{-16}$ | 2.22 x $10^{-16}$ | 2.35 x $10^{-30}$ |
| 0.6 | 2.22 x $10^{-16}$ | 2.22 x $10^{-16}$ | 5.53 x $10^{-29}$ |
| 0.7 | 6.66 x $10^{-16}$ | 2.22 x $10^{-16}$ | 1.29 x $10^{-28}$ |
| 0.8 | 1.55 x $10^{-15}$ | 2.22 x $10^{-16}$ | 3.05 x $10^{-28}$ |
| 0.9 | 3.11 x $10^{-15}$ | 0 | 7.59 x $10^{-28}$ |
| 1.0 | 6.66 x $10^{-15}$ | 0 | 2.02 x $10^{-27}$ |
| CPU Time | | | 0.1467 |

TABLE IV: Maximum relative error, rate of convergence and number of function evaluations for OSMDHBM in Example 2

| $h$ | MRE | ROC | $NF_{eval}$ |
|---|---|---|---|
| 0.1 | 1.3600 x $10^{-17}$ | 10.113 | 50 |
| 0.01 | 1.3064 x $10^{-27}$ | 10.002 | 500 |
| 0.001 | 1.3058 x $10^{-37}$ | 10.000 | 5000 |

Table III presents the absolute error at selected points obtained using the OSMDHBM with $h = 0.01$ and twenty iterations on the closed interval [0,1]. The results were compared with the block two-step hybrid methods based on Bhaskara points (BTSHM-BP) [7] and OTSBHM [7] when $\psi = 5$. The OSMDHBM, which uses the fewest intra-step points (three), is superior to BTSHM-BP and OTSBHM. Table IV illustrates the maximum relative error, rate of convergence and number of function evaluations of OSMDHBM for different step sizes on the closed interval [0,1].

TABLE V: Absolute error for Example 3 when $\psi = 3$ at $h = \frac{1}{10}$

| | ADM [17] | ADM [17] | OSMDHBM | OSMDHBM |
|---|---|---|---|---|
| $x$ | $y_1$ | $y_2$ | $y_1$ | $y_2$ |
| 0 | 1 | 0 | 0 | 0 |
| 0.1 | 4.441 x $10^{-16}$ | 2.914 x $10^{-16}$ | 5.505 x $10^{-25}$ | 6.418 x $10^{-24}$ |
| 0.2 | 2.887 x $10^{-14}$ | 2.879 x $10^{-13}$ | 2.338 x $10^{-24}$ | 2.645 x $10^{-23}$ |
| 0.3 | 1.673 x $10^{-12}$ | 1.677 x $10^{-11}$ | 5.618 x $10^{-24}$ | 6.173 x $10^{-23}$ |
| 0.4 | 2.998 x $10^{-11}$ | 3.009 x $10^{-10}$ | 1.068 x $10^{-23}$ | 1.141 x $10^{-22}$ |
| 0.5 | 2.819 x $10^{-10}$ | 2.832 x $10^{-9}$ | 1.787 x $10^{-23}$ | 1.856 x $10^{-22}$ |
| | CPU Time | | 0.0294 | |

TABLE VI: Maximum relative error, rate of convergence and number of function evaluations for OSMDHBM in Example 3

| | MRE | MRE | ROC | ROC | |
|---|---|---|---|---|---|
| $h$ | $y_1$ | $y_2$ | $y_1$ | $y_2$ | $NF_{eval}$ |
| 0.1 | 3.7381 x $10^{-23}$ | 3.4087 x $10^{-22}$ | 10.007 | 10.006 | 200 |
| 0.01 | 3.7319 x $10^{-33}$ | 3.4045 x $10^{-32}$ | 10.000 | 10.000 | 2000 |
| 0.001 | 3.7318 x $10^{-43}$ | 3.4045 x $10^{-42}$ | 10.000 | 10.000 | 20 000 |

Table V shows the computation time and absolute errors obtained using the step size of $h = 0.1$ at selected points within the closed interval [0,1]. The results, as shown in Table V, were compared with the adomian decomposition method (ADM) [17]. These results indicate that the OSMDHBM performs better than ADM in terms of accuracy, yielding smaller errors. The maximum relative error, rate of convergence and number of function evaluations of OSMDHBM for different step sizes within the closed interval [0,1] are displayed in Table VI.

The maximum error, computation time and number of function evaluations of OSMDHBM at different grid points ($R$ = 88, 219, 346) on the closed interval [0,15$\pi$] are displayed in Table VII. The results obtained are compared

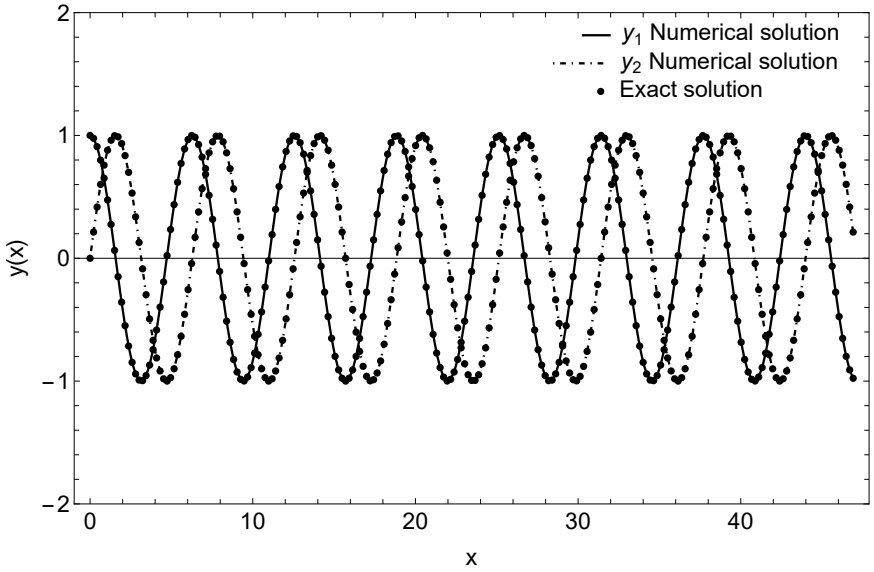


Fig. 5: Numerical vs Exact solution for $y_1$ and $y_2$ when $\psi = 3$ at $R = 219$

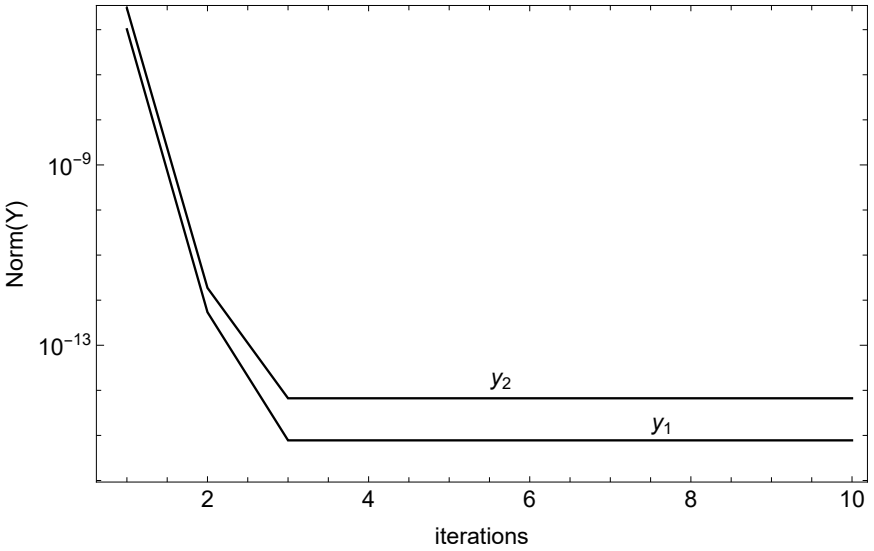


Fig. 6: Convergence graph for $y_1$ and $y_2$ when $\psi = 3$ at $R = 219$

TABLE VII: MAXERR $(max_i|y(x_i) - y_i|)$ for Example 4

| $N$ | Method | MAXERR($y_1$) | MAXERR($y_2$) | NF$_{eval}$ | CPU Time |
|---|---|---|---|---|---|
| 88 | Singla *et al* [14] | 9.636 x $10^{-7}$ | 1.01 x $10^{-6}$ | 352 | |
| | OSMDHBM | 1.021 x $10^{-13}$ | 1.076 x $10^{-13}$ | 1760 | 0.1478 |
| 219 | Singla *et al* [14] | 4.154 x $10^{-9}$ | 4.315 x $10^{-9}$ | 876 | |
| | OSMDHBM | 7.025 x $10^{-14}$ | 8.81 x $10^{-14}$ | 4380 | 0.3708 |
| 346 | Singla *et al* [14] | 2.623 x $10^{-10}$ | 2.732 x $10^{-10}$ | 1384 | |
| | OSMDHBM | 2.063 x $10^{-13}$ | 2.178 x $10^{-13}$ | 6920 | 0.5857 |

with those obtained in [14]. Examining the table reveals that the maximum error is smaller than that of [14], indicating better performance.

Figure 2 shows the absolute error for $y$ in Example 1 for the closed interval [0,6] with $R = 97$. Figure 3 displays the convergence graph of $y$ in Example 2 for the closed interval [0,1] with $h = 0.01$ and twenty iterations. The graph demonstrates that $y$ converges after ten iterations. After achieving convergence, the error norm levels off and does not improve with further iterations. Figure 4 illustrates the numerical and exact solution for $y_1$ and $y_2$ in Example 3 on the closed interval [0,1] with $h = 0.1$. Figure 5 presents the numerical and exact solution for $y_1$ and $y_2$ in Example 4 on the closed interval [0,15$\pi$] with $R = 219$. The convergence graph for $y_1$ and $y_2$ in Example 4 with $R = 219$ and ten iterations on the closed interval [0,15$\pi$] is plotted in Figure 6.

## VII. Conclusion

In this study, a OSMDHBM of order ten has been successfully developed. The method incorporates 3-Ds to directly solve both 2-order L-IVPs and N-IVPs. The N-IVPs are linearized using a MPIM. The analysis confirms that the OSMDHBM exhibits zero stability, consistency, and convergence. To verify the accuracy and efficiency of the method, it has been applied to solve some standard IVPs. The outcomes of these solutions were then compared with those obtained using existing methods (see Table I–VII and Figure 2–6). The outcomes strongly affirm the method's efficiency and accuracy.

## ACKNOWLEDGMENT

The authors are grateful to the University of KwaZulu-Natal, South Africa for assistance.

## REFERENCES

[1] J. C. Butcher, "Numerical methods for ordinary differential equations," *John Wiley & Sons*, 2016.

[2] S. O. Fatunla, "Block methods for 2nd-order ordinary differential equations," *International Journal of Computer Mathematics*, vol. 41, no. 1-2, pp. 55–63, 1991.

[3] T. A. Anake, D. O. Awoyemi, and A. O. Adesanya, "One-step implicit hybrid block method for the direct solution of general second order ordinary differential equations," *IAENG International Journal of Applied Mathematics*, vol. 42, no. 4, pp. 224–228, 2012.

[4] S. N. Jator and J. Li, "A self-starting linear multistep method for a direct solution of the general second-order initial value problem," *International Journal of Computer Mathematics*, vol. 86, no. 5, pp. 827–836, 2009.

[5] O. Adeyeye and Z. Omar, "Solving third order ordinary differential equations using one-step block method with four equidistant generalized hybrid points," *IAENG International Journal of Applied Mathematics*, vol. 49, no. 2, pp. 253–261, 2019.

[6] S. N. Jator and L. Lee, "Implementing a seventh-order linear multistep method in a predictor-corrector mode or block mode: which is more efficient for the general second order initial value problem," *SpringerPlus*, vol. 3, no. 447, 2014.

[7] M. G. Orakwelu, S. Goqo, and S. Motsa, "An optimized two-step block hybrid method with symmetric intra-step points for second order initial value problems," *Engineering Letters*, vol. 29, no. 3, pp. 948–956, 2021.

[8] W. E. Milne, "Numerical solution of differential equations," *John Wiley & Sons*, 1953.

[9] W. H. Enright, "Second derivative multistep methods for stiff ordinary differential equations," *SIAM Journal on Numerical Analysis*, vol. 11, no. 2, pp. 321–331, 1974.

[10] G. K. Gupta, "Implementing second-derivative multistep methods using the nordsieck polynomial representation," *Mathematics of Computation*, vol. 32, no. 141, pp. 13–18, 1978.

[11] P. Tumba, J. Sabo, and M. Hamadina, "Uniformly order eight implicit second derivative method for solving second-order stiff ordinary differential equations," *Academic Journal of Applied Mathematical Sciences*, vol. 4, no. 5, pp. 43–48, 2018.

[12] M. A. Rufai, A. Shokri, and E. O. Omole, "A one-point third-derivative hybrid multistep technique for solving second-order oscillatory and periodic problems," *Journal of Mathematics*, vol. 2023, 2023.

[13] Z. Omar and M. F. Alkasassbeh, "Generalized one-step third derivative implicit hybrid block method for the direct solution of second order ordinary differential equation," *Applied Mathematical Sciences*, vol. 10, no. 9, pp. 417–430, 2016.

[14] R. Singla, G. Singh, H. Ramos, and V. Kanwar, "An efficient optimized adaptive step-size hybrid block method for integrating w' = f (t, w, w') directly," *Journal of Computational and Applied Mathematics*, vol. 420, p. 114838, 2023.

[15] S. N. Jator, "A sixth order linear multistep method for the direct solution of second order differential equations," *International Journal of Pure and Applied Mathematics*, vol. 40, no. 4, pp. 457–472, 2007.

[16] M. G. Orakwelu, "Generalised implicit block hybrid algorithms for initial value problems," *PhD thesis, University of KwaZulu-Natal*, 2019.

[17] A. Sadeghinia and P. Kumar, "One solution for the system of second order odes by adm and application of physics problems," *International Journal of Modern Sciences and Engineering Technology*, vol. 2, no. 2, pp. 1–10, 2015.